Title

Modular regulation of the stem cell transcriptome defines self-renewal, differentiation, and dedifferentiation

Authors

Amelie Raz[1], Hafidh Hassan[1], Yukiko Yamashita[1,2,3]*

Affiliations

[1]Whitehead Institute for Biomedical Research, 455 Main St, Cambridge MA 02142

[2]Department of Biology, Massachusetts Institute of Technology, 31 Ames Street Cambridge MA, 02142

[3]Howard Hughes Medical Institute, 455 Main St, Cambridge MA 02142

*corresponding author (yukikomy@wi.mit.edu)

Summary

Adult stem cells maintain tissue homeostasis by balancing self-renewal and differentiation. Stem cells themselves are frequently replenished by dedifferentiation of partially differentiated progeny. It is a paradox how stem cells and progeny retain the same potential to be or become stem cells, while undergoing different trajectories of self-renewal, differentiation, and dedifferentiation. Here, we show that Drosophila male germline stem cells (GSCs) solve this paradox via two parallel mechanisms. First, differentiating progeny (spermatogonia) may maintain dedifferentiation-competence by inheriting the transcriptome from GSCs in the form of perdurant mRNA, without actively transcribing these genes. Second, two niche signaling pathways (Bmp and Jak-Stat) activate overlapping but distinct subsets of transcriptional targets, and their combinatorial activity allows equally-potent cells to choose different trajectories. Together, this study reveals how a pool of dedifferentiation-competent progeny is maintained to regenerate stem cells as needed without resulting in tumorigenic stem cell overproduction.

Introduction

Adult stem cells maintain tissue homeostasis by continuous production of differentiated cells. However, stem cells can be lost to damage. Thus, mechanisms to replace stem cells are critical for long-term tissue homeostasis. Dedifferentiation serves as one such replacement mechanism, in which the process of differentiation is reversed to generate stem cells from partially or fully differentiated progeny[1]. Dedifferentiation has been observed in stem cell lineages of the intestine[2], germline[3–5], hair follicle[6], liver[7,8], neuron[9], muscle[10], airway epithelium[11], and others. In a system that uses dedifferentiation, stem cells, differentiating cells, and dedifferentiating cells share the same stemness potential – i.e., the ability to be or become stem cells. However, each of these cells has distinct trajectories of self-renewal, differentiation, and dedifferentiation. It is critically important to separate cells' potential (e.g., ability to dedifferentiate) from trajectory (e.g., actual dedifferentiation activity) to ensure stem cell maintenance while preventing tumorigenic overproliferation of stem cells[12]. How cells maintain the same potential while being on different trajectories remains poorly understood, despite the importance of this process to maintain tissue homeostasis.

The male gonads of the fruit fly *Drosophila melanogaster* are an ideal model for studies of stem cell regulation. The adult Drosophila male germline is composed of germline stem cells (GSCs) and their differentiating progeny, all of which are present in a spatial-temporal order along the length of the adult testis (**Fig 1A**). At the apical tip of the testis, a cluster of somatic cells called the hub serves as the GSC niche. Because GSCs are directly attached to the hub cells, they specifically receive signaling ligands secreted from the niche, primarily in the form of Bmp and Jak-Stat ligands[13]. GSCs simultaneously self-renew and generate a differentiating daughter through asymmetric division, with the mitotic spindle oriented perpendicular to the hub-GSC interface[14]. After division, the hub-proximal daughter cell remains a GSC. The other daughter is displaced from the hub and becomes a differentiating spermatogonia. Spermatogonia of each differentiation stage can be easily distinguished morphologically, based on their 'connectivity', because spermatogonia divide with incomplete cytokinesis. Spermatogonial divisions yield cysts of 2, 4, 8, or 16 interconnected spermatogonia (each called 2-cell spermatogonia, 4-cell spermatogonia, etc (**Fig 1A**). Spermatogonia before the first mitotic division, i.e. '1 cell spermatogonium' is also called gonialblast. These cells migrate further from the niche while mitotically dividing, eventually entering meiosis and completing differentiation to become mature sperm.

The Drosophila testis is a foundational model for *in vivo* differentiation[15]. Upon experimental depletion of GSCs, spermatogonia were observed to dedifferentiate *en masse* to occupy the empty niche, restoring the GSC pool[16–19]. Early spermatogonia (1-2 cell spermatogonia) comprise the majority of dedifferentiation events, with late spermatogonia (4-16 cell spermatogonia) dedifferentiating less frequently[5]. Dedifferentiation of spermatogonia is required for the maintenance of GSC populations long-term even in unperturbed tissues[5,18], resulting in >40% of GSCs being generated from dedifferentiation by the end of the animal's lifespan[20]. Although spermatogonia are capable of dedifferentiation (i.e., they maintain the potential to become GSCs), GSCs and spermatogonia exhibit quite distinct cell biological behaviors[21–26], reflecting their distinct trajectory to self-renew vs. differentiate, respectively. For example, GSCs divide asymmetrically, pinching off the differentiating daughter through complete cytokinesis[26,27]. By contrast, spermatogonia divide symmetrically and remain connected with sister cells via incomplete cytokinesis while differentiating[26,27]. It remains unknown how GSCs and spermatogonia maintain the same potential to be or become stem cells, while being on distinct trajectories and exhibiting different behaviors.

Here, we reveal two parallel mechanisms that maintain GSC homeostasis by dynamically balancing self-renewal, differentiation and dedifferentiation. First, through analysis of single-cell RNA sequencing, we find that GSCs and early spermatogonia share an indistinguishable transcriptome, which we call the "early germ cell transcriptome" or "EGTome". Yet, GSCs can be distinguished from spermatogonia by active transcription of the early germline transcripts (EGTs) that constitute the EGTome. This may provide spermatogonia with a time window in which they preserve GSC potential through maintenance of EGT mRNAs, while simultaneously progressing through differentiation associated with halting EGT transcription. Second, the choice of trajectory (self-renewal, differentiation, or dedifferentiation) by equally-potent cells is determined by combinatorial activity of Bmp and Jak-Stat ligands. Reception of both, neither, or Bmp ligand alone each yields a distinct trajectory: self-renewal, differentiation, or dedifferentiation, respectively. We propose that separation of potential and trajectory via perdurance of transcriptome and use of modular transcriptome via multiple signaling pathways serves as a key mechanism to sustain stem cells while avoiding tumorigenic stem cell overproliferation.

Results

Identification of GSC-enriched transcripts with single-cell RNA sequencing

Cell identity is generally thought to be determined by a specific transcript profile. However, no GSC-specific transcript has been identified to date[28]. Thus far, single-cell and single-nucleus RNA sequencing have identified a cluster of early germ cells that contains a mixture of GSCs and early spermatogonia[28]. We attempted to distinguish GSCs from spermatogonia by further analyzing transcriptional heterogeneity within this earliest germ cell cluster. In all, we performed single-cell sequencing of over 51,000 quality-controlled cells across six biological replicates of dissociated testes (see methods, **Supp Fig 1**). Clustering[29] first yielded distinct superclusters representing the primary cell types present in the tissue, including germline and somatic subpopulations (pigment cells, epithelium, and encapsulating cyst cells) (**Fig 1B**, **Supp Fig 1A-B**). Further clustering of the germline partition, alongside pseudotemporal trajectory inference[29], revealed subclusters with gene expression profiles indicating continuous differentiation from stem cells to mature spermatids (**Fig 1C**, **Supp Fig 1A-E**). Cells at the root of the trajectory (circled and salmon-colored in **Fig 1C**) represent germline stem cells and their recent progeny. By extracting these cells and performing a final round of subclustering, we identified the smallest clusters that could be robustly computationally identified (see **Methods**). Then, to compare the very earliest cluster (**Fig 1D**, brown) with the second-earliest cluster (**Fig 1D**, magenta), we performed single-cell differential expression (SCDE) analysis optimized for low cell counts[30],. Through this strategy, we identified many transcripts with expression restricted to the earliest germ cells in our dataset (**Fig 1E, Table S1**). These transcripts, referred to collectively as “early germline transcripts” (EGTs), included factors that had not been previously described in the male germline, and several of which encode for transcription factors or RNA binding proteins that regulate cell identity in other contexts[31–33].

To determine if the earliest computation cluster represented GSCs, we examined the expression patterns of several EGTs (*ovo*, *stg*, *cher, esg*, *Mov10*, *Pxt*, and *Drep2*)[31,33–38] using RNA fluorescent *in situ* hybridization (FISH). All of these transcripts were expressed in early germ cells including GSCs and 2-cell spermatogonia, but diminished in 4- and 8-cell spermatogonia (**Fig 1F-H**). This is the most restricted transcriptome reported to date for GSCs and their immediate progeny, compared to previously identified ‘GSC-enriched factors’, such as *nanos,* that exhibit mRNA distribution through 8-cell spermatogonia[39] (**Fig 1G-H**). Notably, however, no EGTs were restricted to GSCs alone, suggesting that GSCs may not have a unique transcriptome, and instead share their transcriptional profile with early spermatogonia.

Active EGT transcription distinguishes GSCs from early spermatogonia

The above results revealed that GSCs and their early progeny (through 2-cell spermatogonia) likely share the same early germ cell transcriptome (EGTome), and these two cell types may not be distinguishable via transcript presence. However, it is well-established that the transcription factors of the Bmp and Jak-Stat pathways (Mad and Stat, respectively) (**Fig 2A**) are restricted to GSCs and daughter cells that have not yet separated from the GSC mother[40–42] (as confirmed in **Fig 2B-C**). In the absence of ligand reception, Mad and Stat are not localized to the nucleus and are therefore not active as transcription factors; conversely, upon ligand reception, Mad and Stat localize to the nucleus and drive gene expression[43,44]. If Mad and Stat are responsible for the expression of EGTs, EGTs' active transcription may be limited to GSCs, even if mRNAs are inherited and maintained in spermatogonia.

Consistent with this notion, we found that the nascent transcript of EGT *Drep2* was limited to GSCs, suggesting that active transcription of EGTome may be limited to GSCs. Nascent transcripts can be specifically identified by RNA *in situ* hybridization against intronic sequences. Of the EGTs (**Figure 1E**), only *Drep2* had a sufficiently long intron to successfully visualize intronic RNA through single-molecule RNA FISH (**Fig 2D**). Intronic RNA FISH was combined with exonic RNA FISH to compare the presence of nascent transcription vs. mature mRNA. Notably, intronic *Drep2* signal was strongly restricted to the nuclei of GSCs alone, whereas exonic signal was present in the nucleus and cytoplasm of GSC and early spermatogonia (high expression through 2-cell spermatogonia, and low expression in 4-8 cell spermatogonia) (**Fig 2D-E**). These observations are consistent with a model in which EGTs are actively transcribed in GSCs and inherited by early spermatogonia. Similar transcript perdurance from GSCs to spermatogonia has been previously shown for *nanos* mRNA[39]. Taken together, we propose that maintenance of the EGTome without active transcription may allow early spermatogonia to maintain the potential of dedifferentiation while in the process of committing to differentiation (**Fig 2F**). Such early spermatogonia (1-2 cell spermatogonia) have indeed been shown to be especially dedifferentiation competent relative to later (EGT-negative) spermatogonia[5,45], suggesting that early spermatogonia may more readily dedifferentiate because of their maintained EGTome.

Active transcription of EGTs is largely regulated by the niche signaling

Although GSC-specific active transcription could only be shown for *Drep2* due to the lack of sizeable introns within other EGTs, we found that most of EGTs are upregulated by the activation of Bmp or Jak-Stat pathway (**Fig 3A-D**), suggesting that transcription of EGTs is

indeed regulated by the niche signaling. It is well-established that Dpp overexpression results in tumorous overproliferation of spermatogonia-like cells (referred to as Bmp tumors hereafter)[46], whereas Upd overexpression results in massive overproliferation of GSC-like cells (referred to as Jak-Stat tumors hereafter)[47]. In these tumorous testes, we found that the majority of EGTs are indeed upregulated (**Fig 3A-D**), supporting our hypothesis that active transcription of EGTs is restricted to GSCs with active Bmp and/or Jak-Stat signaling. *ovo* transcript, which was found to be activated by Jak-Stat pathway, was present through the two-cell spermatogonia, outlasting Stat activation; this further supports the notion that EGTs are maintained in early spermatogonia via perdurance of RNAs (**Fig 3E**). Two EGTs (*esg* and *cher*) were not upregulated either by Bmp or Jak-Stat activation, and may require both signaling pathways or an alternative mechanism of promoting transcription (**Fig 3D**). Taken together, these results suggest that the majority of the EGTome is transcribed in response to GSC-limited niche signaling, and that GSCs and spermatogonia are distinguished by niche-dependent active transcription of EGTome.

Bmp and Jak-Stat signaling act independently to define GSC identity

Surprisingly, we found that Bmp and Jak-Stat tumors differed in their EGT expression profiles. For example, some EGTs (e.g. *Mov10*) were upregulated only in response to Bmp activation, whereas others (e.g. *ovo*) were upregulated only in response to Jak-Stat (**Fig 3A-D, Supp Fig 2A)**. Yet, other EGTs (e.g. *stg*) were upregulated in response to either Bmp activation or Jak-Stat activation. These results suggest that the Bmp and Jak-Stat pathways activate overlapping but distinct subsets of the EGTome and operate independently, rather than redundantly.

Supporting the idea that Bmp and Jak-Stat signaling act independently, previous studies have also suggested that each pathway likely regulates distinct aspects of GSC behaviors, although there may be some cross-talk between these two pathways[48]. Specifically, prior work has shown that the tumor phenotypes induced by overexpression of Upd and Dpp differ significantly from each other[40,47,49]. For example, Bmp tumor and Jak-Stat tumor cells demonstrated distinct morphology of the ‘fusome’, the membranous structure that bridges the cytoplasm of differentiating germ cells and has been used to assess the state of germ cell differentiation[26,27] (**Supp Fig 3A**). Whereas Jak-Stat tumors had ‘spherical fusomes’ (or ‘spectrosome’), Bmp tumors exhibit highly branched fusome morphology spanning large germ cell cysts, indicating that these tumor states are distinct (**Supp Fig 3A**). Mirroring the different states of connectivity, germ cells in Jak-Stat tumors divide asynchronously from their neighbors, whereas germ cells in

Bmp tumors share cytoplasm within a cyst and therefore divide synchronously within cysts (**Supp Fig 3B**).

Independence of Bmp and Jak-Stat pathway was further confirmed by the near-lack of mutual activation by the two pathways: Overexpression of Bmp ligand Dpp caused germ cell tumors with Mad$^+$ cells far from the niche (**Figure 4A**), without activating Stat in these tumors (**Fig 4B**); the only Stat+ cells are juxtaposed to the hub cells, likely due to the endogenous niche-secreted Upd ligand). Likewise, overproliferated germ cells caused by Upd overexpression (Jak-Stat tumor) exhibited only a small number of Mad-positive germ cells, mostly around hub-like structures (**Figure 4C**). In these same Jak-Stat tumors, almost all germ cells were positive for Stat (**Fig 4D**). These results suggest that the Bmp and Jak-Stat pathways indeed act independently. Moreover, we found that overexpression of the Jak-Stat ligand Upd does not require Bmp activity to form a tumor. In simultaneous RNAi of the Bmp receptor Thickveins (Tkv) (*tkv*^{RNAi}) and overexpression of Jak-Stat ligand Upd, tumors comprised of GSC-like cells formed, just as they do in overexpression of Upd alone (**Supp Fig 4A-B**). These *tkv*^{RNAi}, Upd-overexpression tumor did not display nuclear Mad in any germ cells, confirming effective knockdown of *tkv* (**Supp Fig 4B**). Thus, germ cell reception of Bmp signaling is not required for the formation of the Jak-Stat tumor.

Simultaneous overexpression of Dpp and Upd resulted in tumors containing many Mad$^+$ cells (**Fig 4E**) and Stat$^+$ cells (**Fig 4F**). Moreover, simultaneous expression of Bmp ligand Dpp and EGT *ovo*, which is responsive to Jak-Stat but not Bmp signaling, resulted in enhancement of Bmp-induced tumor phenotype. Whereas Bmp tumors are typically comprised of spermatogonial-like cells with 32-64 germ cells per cyst, as previously shown[46] (**Fig 4G**), simultaneous overexpression of Ovo and Dpp led to a larger testis with an increase in the number of germ cells found in each cyst (**Fig 4G-H**). Thus, addition of a Jak-Stat target, or Jak-Stat signaling itself, enhances the Bmp tumor phenotype rather than acting redundantly with the Bmp pathway. Together, these data suggest that Bmp and Jak-Stat signaling synergistically define germ cells' behavior.

Bmp-high, Jak-Stat low state defines dedifferentiation

The results thus far suggest that EGTome is regulated modularly by Bmp and Jak-Stat pathways, potentially permitting different outcomes based on reception of both, neither, or only one ligand. Combinations of signaling modules may enable equipotent cells (i.e. GSCs and

spermatogonia) to choose between self-renewal, differentiation, and dedifferentiation. We found that, whereas GSCs are defined by Mad$^+$ and Stat$^+$ (double positive) state and differentiating cells are defined by Mad$^-$ Stat$^-$ (dual negative) state, the Mad$^+$ Stat$^-$ state corresponds to dedifferentiation. When mass dedifferentiation was induced by transient ectopic expression of the differentiation factor Bam[16,17] (*nos-gal4*, *tubulin-gal80, UAS-bam*, see method) (**Supp Fig 5A-B),** dedifferentiating spermatogonia that have not made attachment to hub cells had high Mad signal, whereas they are not yet positive for Stat (**Figure 5A, Supp Fig 5C**). In control conditions in which spermatogonia are not massively dedifferentiating, spermatogonia were Mad- and Stat- negative. These results suggest that EGTs downstream of Bmp might be associated with dedifferentiation. Indeed, expression of Bmp-sensitive transcript *stg* (**Supp Fig 2A, Fig 3A**) was also upregulated in later spermatogonia in dedifferentiation conditions as compared to control conditions (**Fig 5B**). By contrast, expression of *ovo*, which is a Jak-Stat-regulated EGT (**Supp Fig 2A, Fig 3A**), was not changed in dedifferentiation conditions (**Fig 5B**).

We previously found that depletion of the RNA-binding protein Me31B resulted in mass dedifferentiation[39] and this was associated with upregulation of Mad – but not Stat[39]. Recapitulating the results from dedifferentiation arising from GSC loss (**Fig 5B**), we found that *me31b* knockdown likewise led to upregulation of *stg* (Bmp responsive EGT) but not *ovo (*Stat responsive EGT) in spermatogonia, suggesting that *me31b* RNAi recapitulates natural dedifferentiation with the activation of Bmp signaling and resulting transcript expression to promote spermatogonial dedifferentiation (**Supp Fig 5D**). Together, these data suggest that Bmp signaling and the resulting transcriptional output is a hallmark of spermatogonial dedifferentiation in both conditions of GSC loss and genetic perturbation.

Consistent with the notion that “Bmp on, Stat off” triggers dedifferentiation in spermatogonia that have not yet contacted the niche, the combination of Stat-off (*nos>stat^{RNAi}*), Bmp-on (*nos>dpp*) resulted in high levels of dedifferentiation (**Fig 5C**). Dedifferentiation can be identified by the presence of hub-proximal spermatogonial cysts of ≥3 germ cells connected by fragmenting fusomes[17,39]. By contrast, differentiating spermatogonia typically have branched, continuous fusomes that connect all cells of the cyst[50]. Notably, the high proportion of dedifferentiation observed under Stat-off, Bmp-on condition (*nos>stat^{RNAi}, dpp*) was likely not due to the loss of GSCs alone. Although low Jak-Stat signaling alone triggered partial GSC loss as reported previously[17] (**Supp Fig 5E**), spermatogonial cysts attached to the hub under these conditions contained a branched fusome, indicative of differentiation, instead of dedifferentiation (**Supp Fig**

5E-H). This suggests that increased dedifferentiation found in Bmp-high, Jak-Stat-low conditions was not merely due to GSC loss from *stat*^{RNAi}, but due to dedifferentiation triggered by Bmp overexpression. Although it was suggested that Jak-Stat activity promotes dedifferentiation[16,17], the fact that Stat was never observed in dedifferentiating SGs that have not made contact with the hub may suggest that Stat is required to reestablish GSC identity upon returning to the niche, rather than initiating dedifferentiation. Consistent with this notion, in Bmp-high, Jak-Stat-low testes, Bmp-sensitive transcripts were expressed outside their normal GSC/early SG expression boundary; Bmp-insensitive transcripts, by contrast, retained their normal expression pattern (**Supp Fig 5I**). Together, these data suggest that a Bmp-high, Jak-Stat-low environment is sufficient to trigger dedifferentiation.

Discussion

The plasticity of adult stem cell populations, and the ability of partially differentiated cells to re-acquire stem cell character, has been increasingly recognized in diverse adult stem cell populations[1]. In such a dynamic system, stem cells and differentiating cells *en route* to terminal differentiation must balance competing demands. Stem cells must remain distinct from their daughter cells, with a unique self-renewal trajectory and associated cell biological behaviors that support self-renewal. Differentiating cells must maintain stem cell potential even while adopting a differentiation trajectory. Our work revealed two parallel mechanisms to separate potential and trajectory (**Fig 5D**). First, our data suggest that stem cells are the only germline cells that actively transcribe the early germline transcriptome, whereas differentiating cells share the same set of transcripts as stem cells by inheriting them but not actively transcribing them. This may provide differentiating cells with the potential to revert back to stem cell identity without causing tumorous overproliferation. Second, dual niche signaling allows cells to define more than two states (self-renewal and differentiation), enabling cells to define the third state (dedifferentiation) when only one niche signaling (Bmp) but not the other (Jak-Stat) is on. Thus, we propose that transcriptome regulates potential, whereas the dual niche signaling enables distinct trajectories (self-renewal vs. differentiation vs. dedifferentiation).

Importantly, our study demonstrates both the benefits and limitations of using single-cell sequencing to categorize cell types. While such sequencing was vital to define the EGTome, without which it would be impossible to determine if Bmp and Jak-Stat signaling have distinct sets of targets, it also failed to distinguish GSCs and spermatogonia. Incomplete or incorrect inferences of cell type from transcriptomic studies are often attributed to translational

regulation[51]. It awaits future investigation to test if EGTs are differentially translated or undergo different post-translational control in GSCs and spermatogonia. Indeed, restriction of Mad and Stat to GSCs likely occurs post-translationally[43,44], and recent work has identified that translational control serves as a key regulator to distinguish somatic stem cells and their progeny[52]. Our study, however, suggests that 'active transcription', controlled by transcription factor activity, is an important parameter of cells' state. Whereas GSCs and early spermatogonia share a transcriptome (EGTome), GSCs are likely the only cell type that is actively producing EGTome, revealing an important limitation of single-cell transcriptomic analysis in isolation.

Previously, we showed that GSCs are likely the only cells that can receive Bmp ligand secreted by the hub under normal conditions[53]. GSCs extend membranous protrusions (called microtubule-based nanotubes, or MT-nanotubes) into the hub cells, and the interface between the MT-nanotubes and the hub cell invaginations serves as the only site for productive ligand-receptor interaction. Therefore, spermatogonia displaced from the hub are excluded from engaging in the niche signaling[53]. The very presence or absence of GSCs could therefore determine the ability of spermatogonia to receive Bmp ligand. The Jak-Stat ligand Upd, by contrast, is known to be diffusion-limited through its association with the extracellular matrix[54], and is likely never receivable by spermatogonia distal from the hub, regardless of presence or absence of GSCs. This allows for a precisely controlled emergent phenomenon, in which spermatogonia in the presence of GSCs do not receive a high Bmp signal and therefore do not activate a dedifferentiation program. By contrast, in the absence of GSCs, Bmp ligand may diffuse and reach spermatogonia, initiating an active transcriptional program associated with dedifferentiation initiation. Upon homing to the niche (i.e. reestablishment of attachment to the hub), such dedifferentiating spermatogonia will reactivate Jak-Stat signaling, thus returning to the true GSC state (by reacquiring GSC behavior and/or suppressing dedifferentiation-specific behavior such as migration).

A recent study[55] proposed that Bmp ligand diffusion during homeostasis suppresses, rather than promotes, differentiation of the spermatogonia. Specifically, trapping Bmp ligand to the hub cell surface increased, rather than decreased, the frequency of spermatogonia dedifferentiating into GSC identity. Because Bmp ligand is known to exert distinct effects depending on its concentration[56], trapping ligand on secreting cells may create a state of Bmp signaling in the spermatogonia distinct from direct perturbations of pathway components. It awaits future

investigation to understand how specific levels of Bmp signaling, potentially in combination with varying levels of Jak-Stat signaling, may encode specific cellular states.

The reactivation of Bmp targets during dedifferentiation has another important implication. Dedifferentiation in an unperturbed tissue to replace sporadic GSC loss is likely supported by dedifferentiation of one- or two-cell spermatogonia, and GSCs may be homeostatically maintained through interconversion with their immediate daughters[5,45]. However, after GSC loss, dedifferentiation of 4-cell spermatogonial cysts is frequently seen[17]. These one- or two-cell spermatogonia differ from 4-cell spermatogonia in terms of number of divisions being a GSC and in distance from the hub. Our work identifies another difference in these populations: high expression of the EGTome. Because our GSC-enriched transcripts are constantly seen in early spermatogonia (**Fig 1** and **Supp Fig 1**), inheritance of EGTome from GSCs may maintain a pool of particularly dedifferentiation-competent 2-cell cysts. By contrast, Bmp-sensitive GSC-enriched transcripts are found after GSC loss in 4-cell spermatogonial cysts (**Fig 5**). Therefore, this *de novo* transcription of Bmp-responsive factors could be particularly critical during mass dedifferentiation after GSC loss, whereas high perdurant transcript levels primarily maintain dedifferentiation competence during homeostasis.

Taken together, this work provides important insights into the puzzle of how stem cell lineages balance self-renewing and differentiating cell populations, while maintaining the opportunity for interconversion between these populations. Maintaining this balance, such that dedifferentiation does not occur too frequently in homeostasis resulting in tumorigenesis, yet can be robustly triggered after GSC loss, is paramount to tissue equilibrium.

Acknowledgments. We acknowledge members of the Yamashita lab for critical input. We thank FlyBase, Bloomington Drosophila Stock Center, and the Drosophila Genomics Resource Center for reagents. YMY was supported in this work by the Howard Hughes Medical Institute and the Gordon and Betty Moore Foundation. AAR was supported in this work by 1F32GM143850-01 and 1K99GM154143-01A1.

Author Contributions. Conceptualization, AAR and YMY; investigation, AAR and HH; analysis, AAR; writing – original draft, AAR; writing – editing, AAR and YMY; funding acquisition, AAR and YMY; supervision, YMY.

Competing Interests. The authors declare no competing interests

Data and materials availability. The single-cell sequencing data is available to reviewers upon request and will be deposited to GEO.

Methods

Fly husbandry and strains. Unless otherwise stated (see "Dedifferentiation Regime"), flies were raised at 25° and assayed at age 1-4 days. All flies were raised on standard Bloomington media without propionic acid. For a list of all fly strains used in this study, see **Table S2.**

Tissue isolation and dissociation for scRNA-seq. Dissociation was performed as previously described[28]. Briefly, on the day of the dissection, fresh dissociation buffer (2 mg/mL collagenase in Trypsin LE) was prepared. Testes from 1-4 day old flies were dissected in 1x phosphate-buffered saline (PBS) and immediately transferred to cold PBS tubes for a maximum of 30 minutes while the remaining dissections were performed. Testis samples were centrifuged at 135 rcf, PBS was removed and replaced with dissociation buffer. Testes were incubated in maceration buffer for 30 minutes with gentle vortexing every 10 minutes at room temperature. Following incubation, samples were pipetted up and down until no visible tissue chunks remained. Sample was then passed through a 35 µm filter and centrifuged at 135 rcf for 7 minutes. The supernatant was removed and the pellet was resuspended in 1 mL of calcium/magnesium-free Hanks' Balanced Salt Solution (HBSS). The sample was centrifuged for a final time at 135 rcf for 7 minutes and all but 50 µL of the HBSS was removed. The pellet was resuspended in the remaining 50 µL. Cell viability and density was assayed on a hemocytometer with DIC imaging and Acridine Orange stain.

Library preparation and single-cell sequencing. Cells were processed using the 10X Genomics Chromium Controller and Chromium Single Cell Library And Gel Bead Kit following standard manufacturer's protocol. Amplified cDNA libraries were quantified by bioanalyzer and size-selected using AMPure beads. Samples were sequenced on a NovaSeq S4

Mapping, dimensionality reduction, clustering, and pseudotime analysis. Reads were mapped to the DM6 reference genome using the 10X CellRanger pipeline with default parameters, on a per-sample basis. The resulting feature matrices for all 6 biological samples were read into the R package Monocle3[29] using load_cellranger_data. The samples were

combined using combine_cds and aligned using align_cds; no other sample integration methods were used. The data was preprocessed using preprocess_cds and dimensionality reduction was performed with reduce_dimensions. Initial partitioning was performed by clustering cells at resolution 1^{-5}. At this point, the germline partition was embedded and a principal graph was generated using learn_graph. The germline partition was then further subclustered with resolution 0.0006 using cluster_cells again. These clusters were then manually merged and recoded, as in Supp Fig 1A. The pseudotime trajectory was inferred using order_cells of the germline partition, with "cluster A" identified as the root. Finally, cluster A was isolated and subclustered one last time at resolution 0.01. Additional subclustering at higher resolutions did not reproducibly generate similar clusters when different random seeds were set; therefore, this was considered the last possible biologically relevant clustering for this dataset.

Identification of EGTs. Because of the low cell count in the final clustering, differential gene expression analysis was performed using the SCDE package that is most reliable for low cell counts[30]. First, an expression matrix was created with "positive" cells (putative GSCs) and "negative" cells (putative spermatogonia) from cell names (colnames) within the cds object. A csv file was generated from the merged feature-barcode matrix in bash the mat2csv command (CellRanger). SCDE was then run as per package defaults. The output file was merged with the original features file to annotate gene short names and FlyBase ID. The hits were sorted by "conservative estimate" (ce). See Table S1 for the full list.

Microscopy and image processing. All microscopy images were taken on a Leica Stellaris using a 63x oil-immersion objective and processed using FIJI. For the 3D reconstruction, the Imaris machine-learning based 3D modeling was used.

Immunofluorescence. Immunofluorscence staining was performed as described previously[20]. Briefly, testes were dissected in PBS, transferred to 4% formalydehyde in PBS and fixed for 30 minutes. Tissues were then washed in PBS + 0.1% Triton X (PBST) for 3 times, 10' each, followed by incubation with primary antibody in 3% BSA in PBST at 4° overnight. Samples were washed in again 3x10' in PBST and incubated in secondary antibody in 3% BSA in PBST. Washes were performed again and samples were mounted in Vectashield with DAPI. The exception to this protocol was for the anti-Mad antibody. For stains with this antibody, two modifications were made. First, initial washes were performed with PBS + 0.3% Triton X prior to incubation in primary. Second, a 30' blocking step in 5% BSA (not 3%) was performed, and the

primary antibody incubation was in 5% BSA. When immunofluorescence was combined with TSA FISH, the FISH protocol was performed first, followed by the immunofluorescence protocol.

TSA FISH. All RNA *in situ* experiments, with the exception of Fig 1G, Supp Fig 2A, and Fig 2C, were performed using tyramide signal amplification (TSA) FISH. RNA oligoprobes were synthesized from Drosophila Genome Resource Center (DGRC) plasmids, as described[57] (**Table S2**). Briefly, plasmids were linearized and amplified as follows: pBS backbone with SK-30 (F) and SKMet (R), pFLC-1 packbone with M13(-21) (F) and M13 (REV) (R), and pOT2a backbone with PM001a (F) and PM002a (R). *in vitro* transcription reactions were performed on the PCR products with the following polymerases: T3 for the pBS or pFLC-1 backbones, and SP6 for the pOT2a backbone. The reactions were performed with Digoxigenin (DIG)-conjugated ribonucleotides (Roche). Following the transcription reaction (overnight at 37°), the reaction was treated with DNase and then probes were precipitated with 7.5M Ammonium Acetate and 100% ethanol, and resuspended in formamide.

FISH with tyramide signal amplification was then performed as described[28]. Testes were isolated and fixed in 4% formaldehyde for 30–60 min, dehydrated into methanol and stored at –20 °C for up to 1 month. After rehydration in PBS +0.1% Triton- X100, testes were permea- bilized with 4 µg/ml Proteinase K for 6 min and washed with Pre- Hybridization solution (50% deionized formamide, 5x SSC, 1 mg/ml yeast RNA, 1% Tween- 20) for up to 2 hr at 56°. Testes were incubated overnight at 56 °C with probes diluted 1:800 in Hybridization solution (50% deionized formamide, 5x SSC, 1 mg/mL yeast RNA, 1% Tween- 20, and 5% Dextran Sulfate). After washes in Pre- Hybridization solution, 2 x SSC, and 0.2 x SSC, then PBS +0.1% Triton- X100, samples were blocked for 30 min in 1% Roche Western Blocking Reagent prior to incubating overnight at 4 °C with either anti- FITC with horseradish peroxidase conjugate (Roche) at a 1:2000 concentration or anti- DIG- with horseradish peroxidase conjugate (Roche) at a 1:1500 concentration in 1% Roche Western Blocking Reagent. Fluorescent tyramide development and amplification were performed by first placing the testes for 5 min in borate buffer (0.1 M boric acid, 2 M NaCl, pH 8.5), followed by 10 min in borate buffer with rhodamine (1:1000) or fluorescein (1:1500) tyramide, and 0.0003% hydrogen peroxide. Samples were washed before continuing to immunofluorescence.

Stellaris FISH. For single-molecule FISH (Fig 1G and Supp Fig 2A), FISH with probes from Biosearch Technologies was performed as previously described[58]. Probes were designed

against the coding sequences of *nanos*, *ovo*, *Mov10*, and *stg* using the Biosearch Technologies design tool. Testes were dissected in 1x PBS and fixed in 4% formaldehyde in 1x PBS for 30 min. Then testes were washed briefly in 1x PBS and permeabilized in 70% ethanol overnight at 4°. Testes were briefly rinsed with wash buffer (2x SSC, 10% formamide) and then hybridized overnight at 37° in hybridization buffer containing 2x SSC, 10% dextran sulfate (Sigma-Aldrich), 1mg/ml Escherichia coli tRNA (Sigma-Aldrich), 2 mM Vanadyl Ribonucleoside complex (NEB), 0.5% BSA (Ambion), and 10% formamide. Fluorescently labeled probes were added to the hybridization buffer to a final concentration of 100 nM. Following hybridization, samples were washed three times in wash buffer for 20 min each at 37°.

HCR FISH. For the nascent transcript FISH on *Drep2* (Fig 2C), we used Hybridization Chain Reaction (HCR) FISH. Using the Molecular Instruments design tool, nascent probes were designed against the third and fourth introns and exonic probes were designed against the coding sequence of *Drep2*. Testes were dissected in 1x PBS and fixed in 4% formaldehyde in 1x PBS for 20 minutes and then washed twice, 5 minutes per wash, in 1x PBS 0.1% Tween-20. Permeabilization was achieved by washing for 2 hours in 1x PBS + 0.1% Triton X-100. The testes were then washed twice, 5 minutes per wash, in 5x SSC + 0.1% Tween-20. Probes were added to Hybridization Buffer to a final concentration of 10nM. Samples were hybridized overnight at 37C shaking. Samples were washed four times, 15 minutes per wash, at 37° with Probe Wash Buffer (Molecular Instruments). During the second wash, hairpin solutions for desired amplifiers (Molecular Instruments) were created by individually heating each hairpin at 95C for 90 seconds in a PCR machine and allowing the samples to slowly cool to room temperature. Amplifiers were added to Amplification Buffer (Molecular Instruments) to a final concentration of 60nM. Samples were washed twice, 5 minutes per wash, with 5x SSC 0.1% Tween-20, and then transferred to Amplification Buffer + amplifiers and incubated overnight at room temperature nutating. Testes were then washed twice, 30 minutes per wash, with 5x SSC 0.1% Tween-20.

Dedifferentiation regime. To generate dedifferentiation conditions by overexpression of Bam in GSCs, we took advantage of the temperature-sensitive Gal80 system to drive Bam. Specifically, *nos-gal4*, *tubulin-gal80* flies were crossed with *UAS-bam* flies and raised at 18°. Upon eclosion, adult *nos-gal4, tubulin-gal80, UAS-bam* flies and their control siblings were transferred to a 29° water bath for 64 hours. This timepoint was empirically determined to provide maximum GSC loss (see Supp Fig 5) without overwhelming spermatogonial loss. Following the 29° incubation,

flies were transferred back to 18° for an additional 64 hours before dissection. This time was likewise determined to allow the maximum number of confident dedifferentiation events.

1 ## Figures

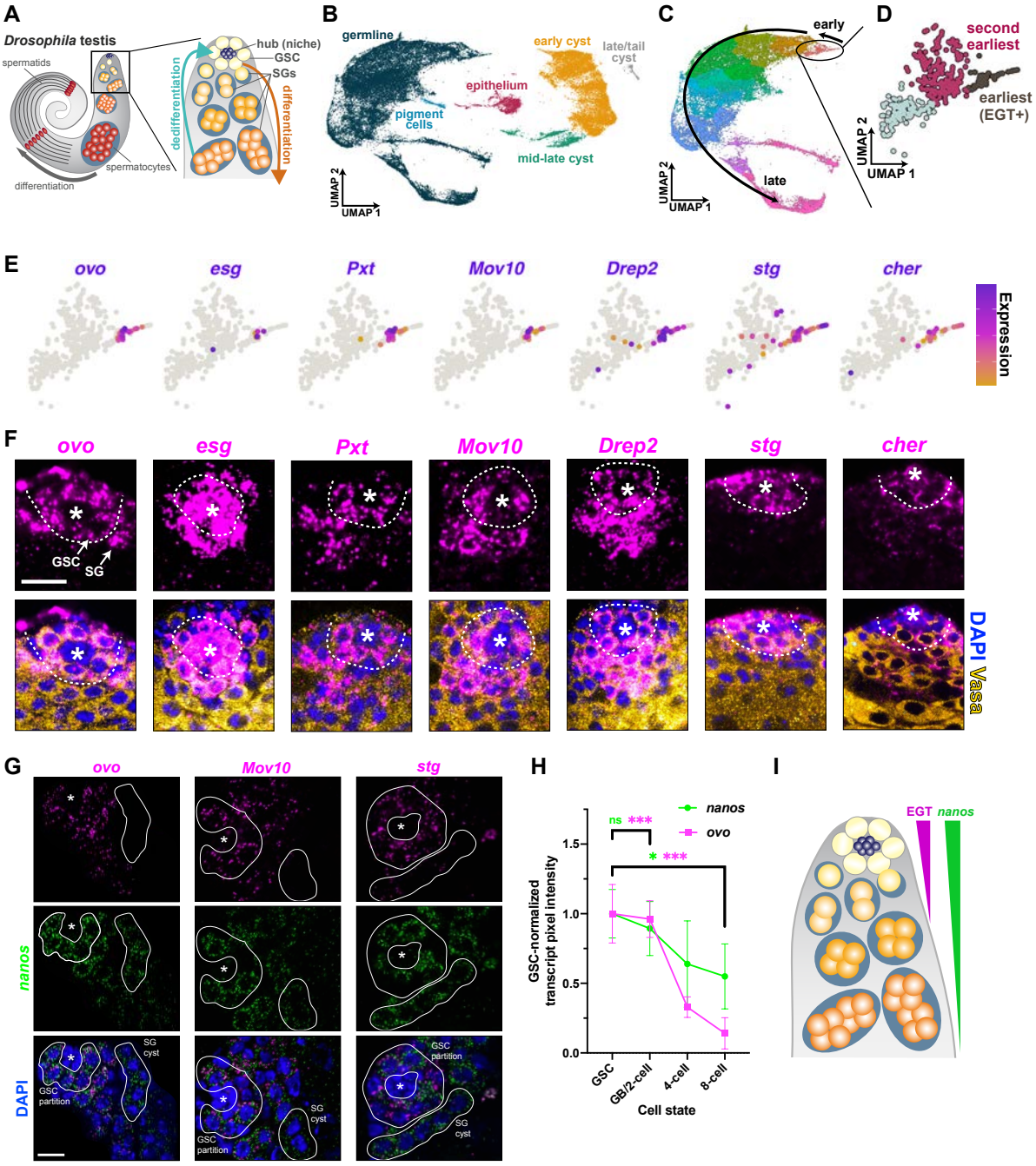

2

3 **Figure 1. Single-cell analysis reveals an early germline transcriptome (EGTome). (A)**
4 Schematic of the Drosophila testis. The adult Drosophila male germline is maintained by
5 germline stem cells (GSCs), which can both self-renew and give rise to differentiating
6 spermatogonia. Spermatogonia divide four times while differentiating, mature into pre-meiotic
7 spermatocytes, undergo meiosis as spermatids, and mature as sperm. Spermatogonia can
8 dedifferentiate to GSCs. **(B)** UMAP representation of all singly sequenced cells in the testis.

Each dot represents a cell, and the proximity of cells to each other approximates closeness in gene expression space. Color denotes broad cluster annotation. **(C)** UMAP representation of all germline annotated cells in the testis. Arrows indicate differentiation direction. The GSCs and spermatogonia (colored salmon and circled) are collectively known as “gonia”. Color indicates merged and quality-controlled germline cluster annotation. **(D)** (top) UMAP representation of gonia, colored by further subcluster. (bottom) Schematic of single-cell differential expression analysis comparing putative spermatogonia (magenta in UMAP plot) to putative GSCs (grey-brown in UMAP plot). **(E)** UMAP plots of gonia with representative early germline transcripts (EGTs) featured. Color indicates expression of gene listed, with blue as highest and orange as lowest detectable. Grey cells have no detectable expression. **(F)** RNA FISH of EGTs in 1E. Asterisk marks the hub. All factors are expressed in GSCs ($Vasa^+$ cells contacting the hub, within the dashed line) and in at least some spermatogonia ($Vasa^+$ cells not contacting the hub, outside the dashed line). Some factors, including *esg, stg,* and *cher* are also expressed in somatic cells. Scale bar, 10 μm. **(G)** Single-molecule FISH of EGTs reveals that they are all more restricted to GSCs than *nanos* transcript, a common GSC-enriched marker. In all images, both dual-positive GSCs and *nanos*-single positive spermatogonia are highlighted. Asterisk marks the hub. Scale bars, 10 μm. **(H)** Quantification of pixel intensity from **(G)**. Error bars, standard error. *, $p<0.01$; ***, $p<0.0001$, unpaired t-test.

See also **Figure S1**.

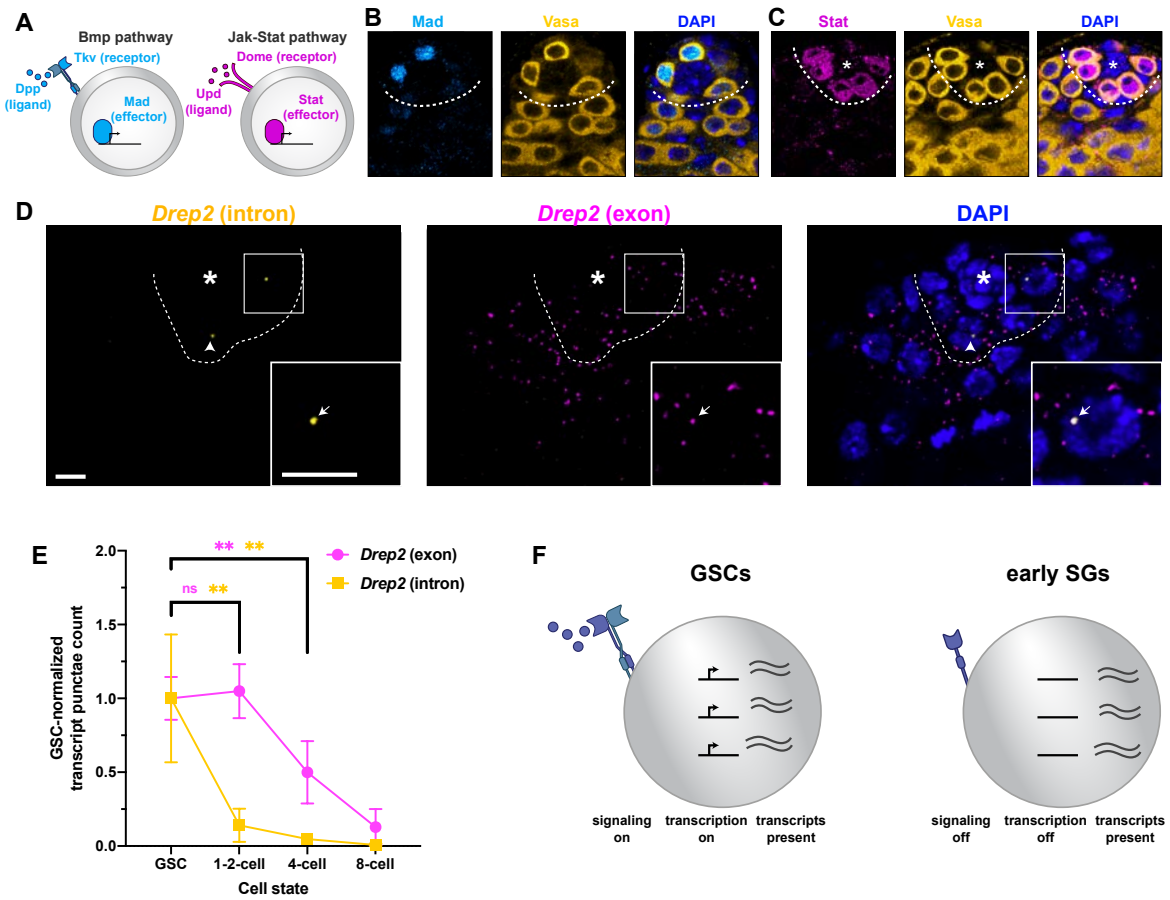

Figure 2. GSCs and spermatognia differ on the basis of active transcriptional state. (A) Model of the Bmp and Jak-Stat pathways in Drosophila. In the Bmp pathway, Dpp (ligand) binds to the receptor Tkv, triggering the nuclear localization of the transcription factor Mad. In the Jak-Stat pathway, Upd (ligand) binds to the receptor Dome, triggering nuclear localization of the transcription factor Stat. **(B)** GSCs, but not spermatogonia, are positive for the Bmp transcriptional effector Mad. Scale bar, 10 μm. **(C)** GSCs, but not spermatogonia, are positive for the Jak-Stat transcriptional effector Stat. Scale bar, 10 μm. **(D)** Nascent transcription can be identified by intronic signal. Intronic signal of EGT *Drep2* is localized to the nucleus of GSCs, whereas exonic signal is present in the nucleus and cytoplasm of both GSCs and spermatogonia. Scale bars, 5 μm. **(E)** Quantification of the data in C. Error bars represent standard error. **, $p<0.001$, unpaired t-test. **(F)** Model of GSC vs. spermatogonia difference. GSCs receive signaling information from the hub, promoting transcription of EGTs. Spermatogonia do not receive signaling and thus do not have active transcription, but retain mature mRNAs transcribed in GSCs.

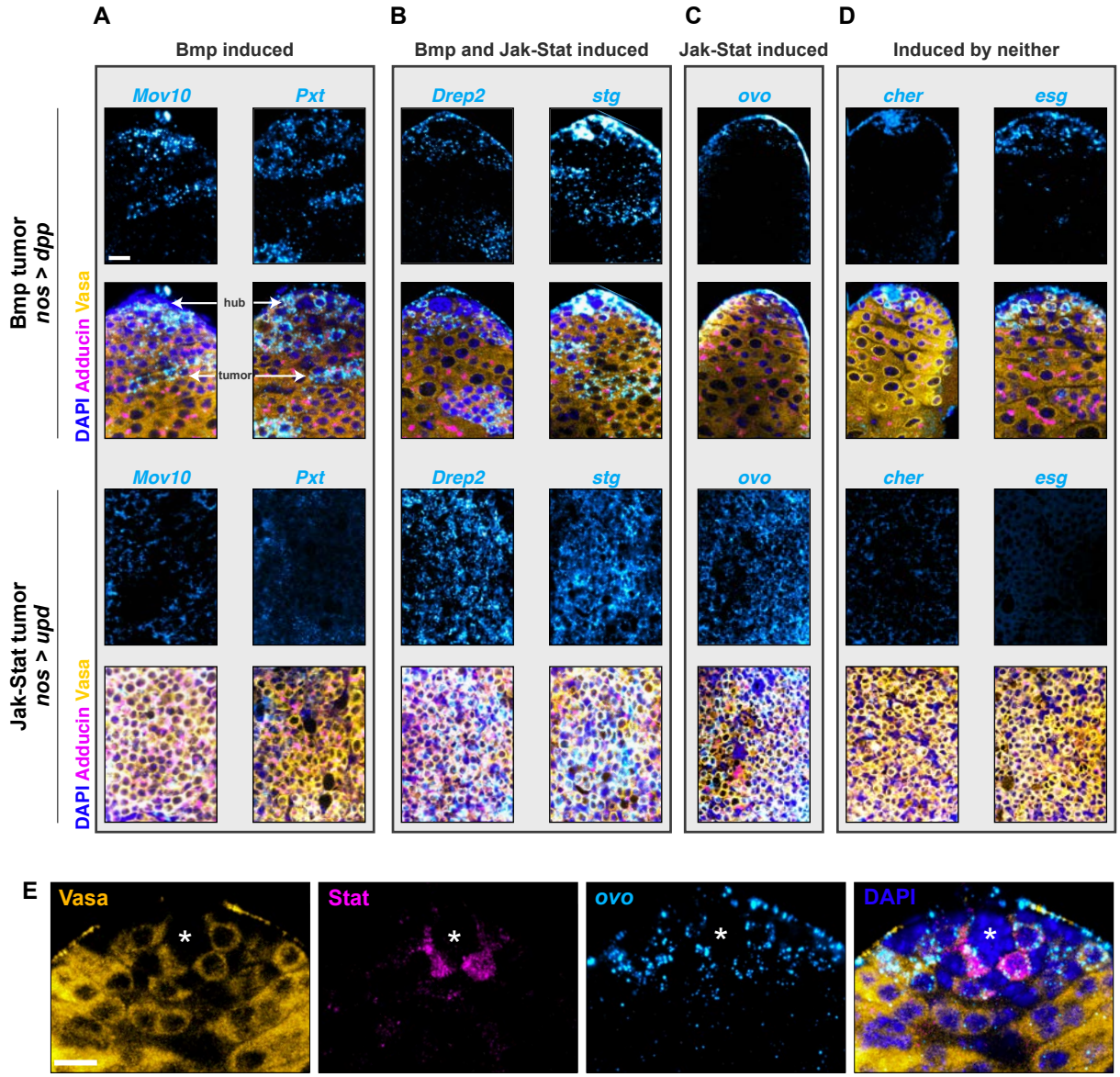

Figure 3. Bmp and Jak-Stat promote separable transcriptional programs. (A-D) EGTs have variable expression in conditions of Bmp vs Jak-Stat upregulation. In these testes, hub-proximal germ cells likely represent GSCs receiving both niche ligands from endogenous niche cells, whereas hub-distal tumor cells arise from upregulation of Bmp signaling or Jak-Stat signaling alone, depending on ectopically expressed ligands. **(A)** *Mov10* and *Pxt* are expressed in Bmp tumors, but not Jak-Stat tumors. **(B)** *Drep2* and *stg* are expressed in both Bmp and Jak-Stat tumors. **(C)** *ovo* is expressed in Jak-Stat tumors, but not Bmp tumors. **(D)** *cher* and *esg* are not expressed in either Bmp or Jak-Stat tumors. **(E)** *ovo* transcript presence perdures past Stat transcription factor presence.

Scale bars, 10 μm.

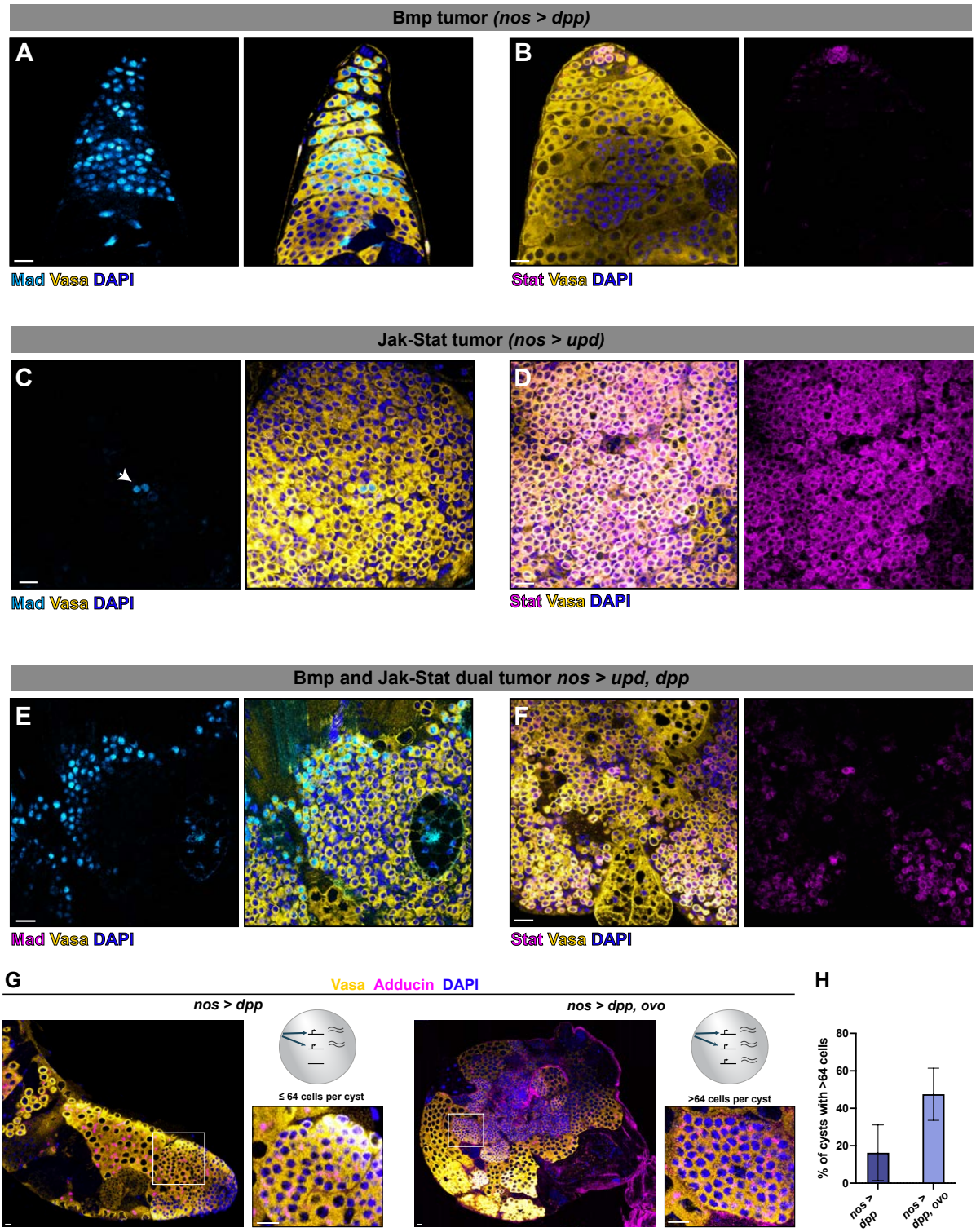

Figure 4. Bmp and Jak-Stat signaling act independently and non-redundantly. (A) Bmp tumor cells distal to the hub are Mad$^+$. Additionally, some somatic cyst cells distal to the hub are Mad$^+$ (arrows). **(B)** Bmp tumor cells distal to the hub are Stat$^-$. Only hub-proximal cells are Stat$^+$.

(C) Most cells in Jak-Stat tumors are Mad$^-$. Mad$^+$ cells in Jak-Stat tumors are located around hub-like structures (arrow). **(D)** Jak-Stat tumor cells largely are Stat$^+$. **(E-F)** Tumors arising from simultaneous overexpression of Upd and Dpp contain many dying or grossly abnormal cells. However, many germ cells are Mad$^+$ **(E)** and/or Stat$^+$ **(F)**. **(G)** Bmp tumors display tumor cysts distal to the hub with up to 64 cells per cyst. In simultaneous overexpression of the Jak-Stat target Ovo, tumors are larger and contain more cells per cyst. Scale bars, 10 μm **(H)** Quantification of cysts containing more than 64 cells, from **(G)**.
Error bars, standard error. Scale bars, 10 μm.

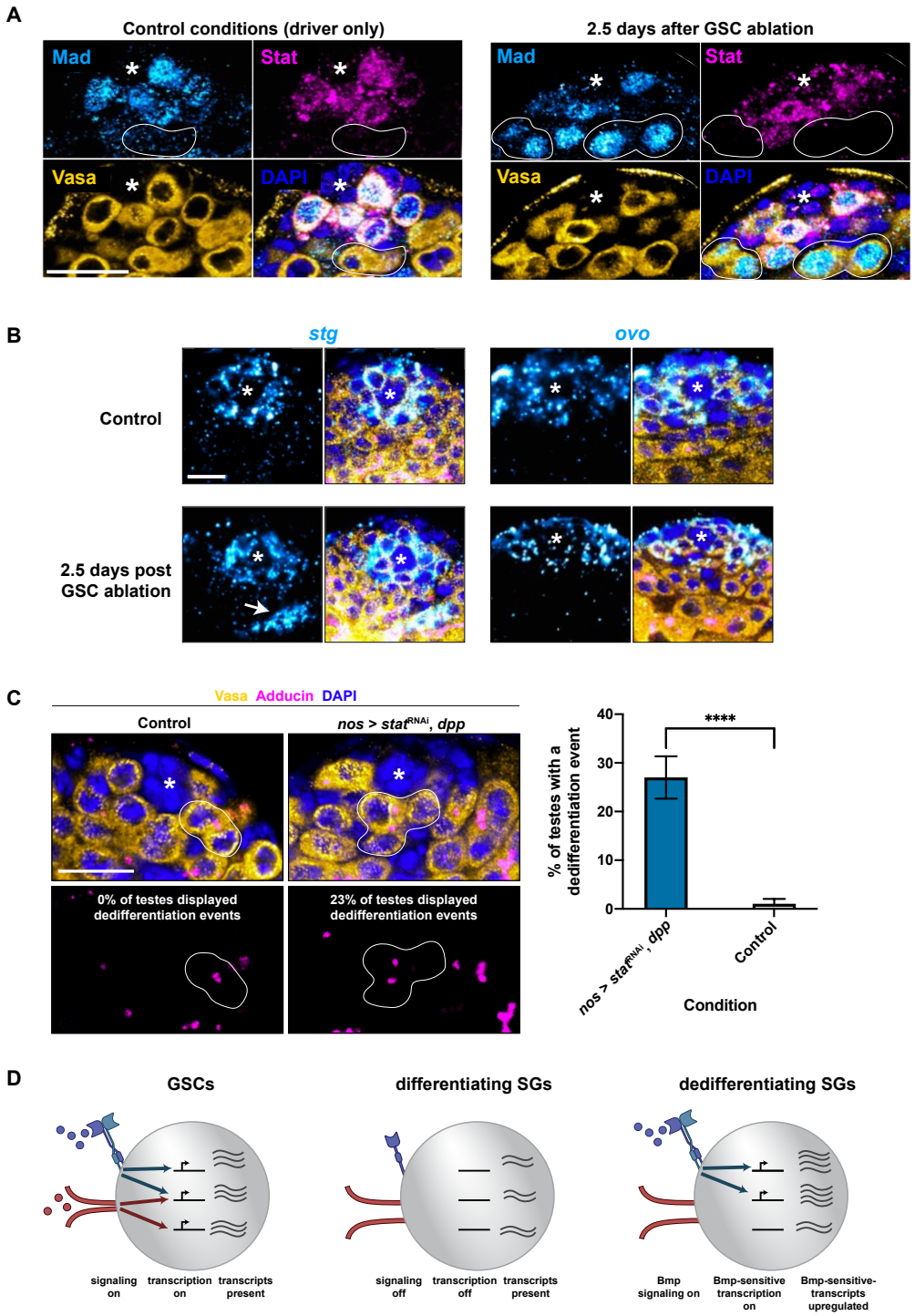

Figure 5. Dedifferentiation is characterized by a Bmp-on, Jak-Stat-off state in spermatogonia. (A) 2.5 days after near-total GSC ablation via transient overexpression of Bam, dedifferentiation is frequent (see **Supp Fig 5A-B**). At this timepoint, spermatogonia (outlined) are Mad$^+$, but not Stat$^+$. **(B)** In control conditions, spermatogonia (outlined) are neither Mad$^+$ or Stat$^+$. **(C)** Bmp-sensitive transcript *stg* is found in later spermatogonia (arrow) in

dedifferentiation conditions, but Bmp-insensitive transcript *ovo* is not. **(D)** Dedifferentiation is characterized by cysts of >2 germ cells with disconnected fusomes contacting the hub. This was observed frequently after simultaneous overexpression of Bmp ligand and RNAi of the Stat transcriptional effector. Outline indicates a dedifferentiating cyst. Error bars, standard error. ****, $p<0.00001$, unpaired t-test.

Scale bars, 10 μm

Supplemental Figures

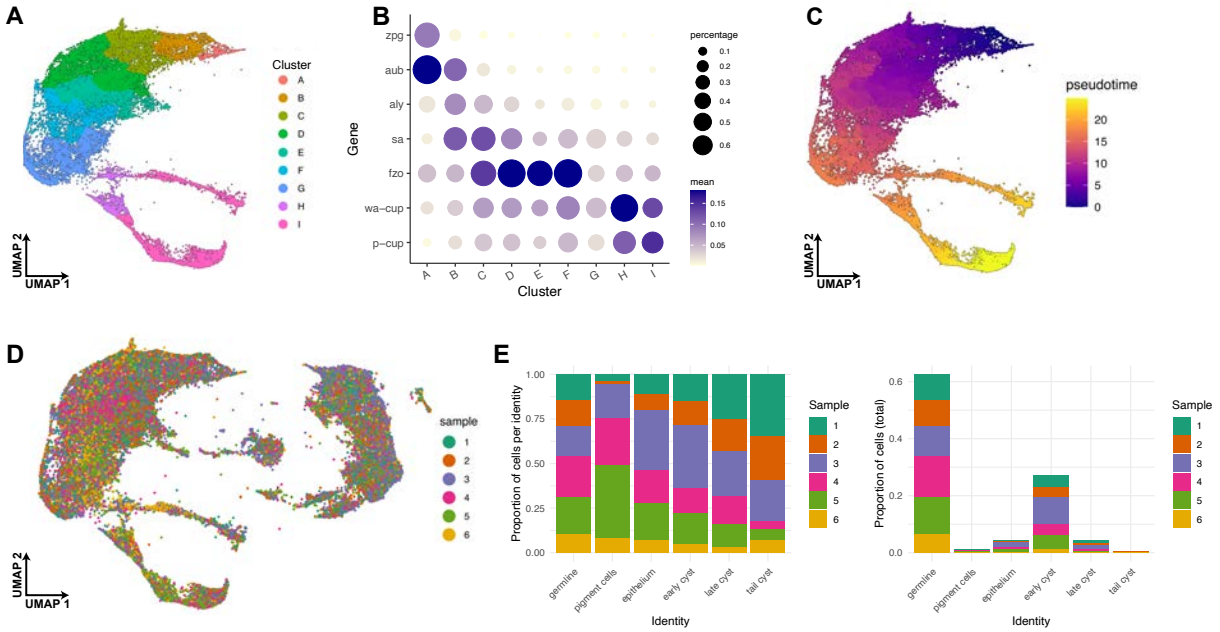

Supplemental Figure 1. Characterization of single-cell sequencing data and validated EGTs. (A) UMAP representation of all germline annotated cells in the testis. Color indicates merged and quality-controlled germline cluster annotation, as in **Fig 1C**. Clusters labeled alphabetically. **(B)** Dotplot displaying clusters, as in **(A)**, with expression of known differentiation-stage markers indicated. Size of dot indicates the percentage of cells in that cluster with an expression level above 0 for that gene. Color indicates the mean expression value across all cells in that cluster for that gene. Transcript presence correlates with known differentiation stages. **(C)** Calculated pseudotime values of germline cells. Germline cells form an unbroken trajectory. Cluster A was imputed as the root. **(D)** UMAP representation of all testis cells. Cells colored by sample from the 6 biological replicates. **(E)** Proportion of cells from each cluster from each biological replicate. Each replicate is represented across all clusters, and outliers are largely only seen in very low-number clusters (pigment cells and tail cyst cells, especially).

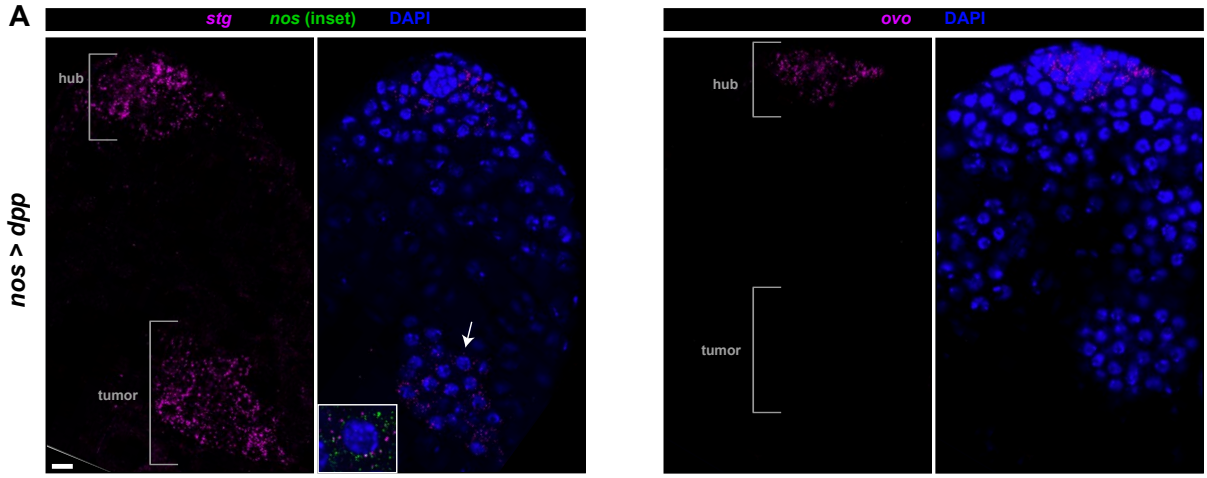

Supplemental Figure 2. Autonomous Dpp signaling promotes a subset of EGTs in germ cells. (A) Single-molecule FISH demonstrates that *stg* is expressed in hub-distal Bmp tumor cells, but *ovo* is only expressed in hub-proximal cells in its normal expression pattern. Tumor expression of *stg* is in *nanos*$^{+}$ germ cells (inset). **(B)** Cyst cells can also receive and react to Dpp. Autonomous Dpp signaling in somatic cyst cells through cell-specific overexpression of a constitutively active Dpp receptor (*thickveins*^{CA}) does not lead to expanded spermatogonial expression of EGTs.

Scale bars, 10 μm.

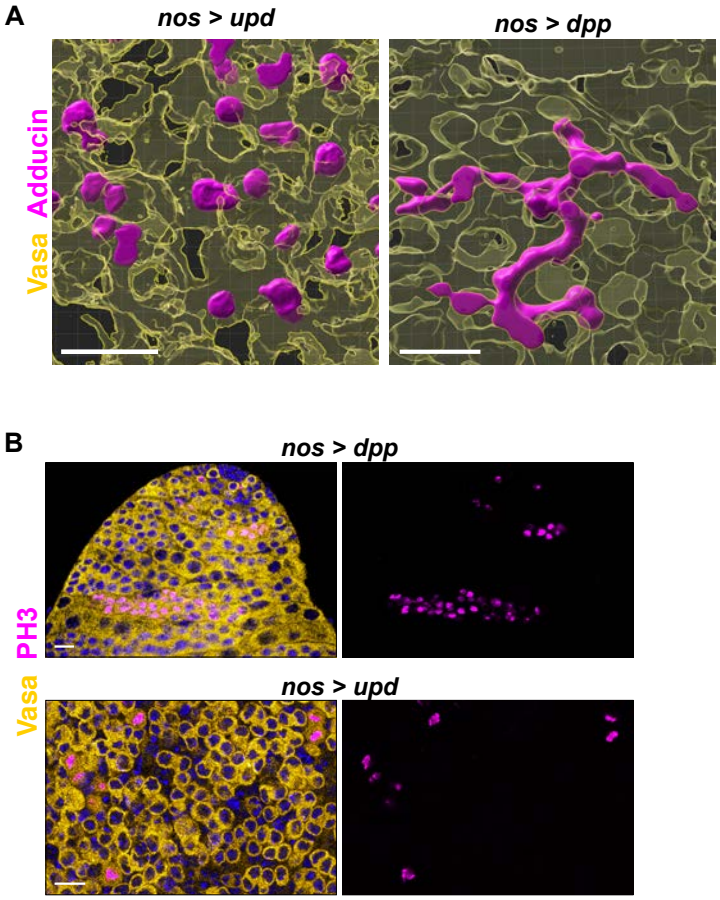

Supplemental Figure 3. Formation of Jak-Stat tumors does not require Bmp signaling. (A) In Jak-Stat tumors, sparse Mad^{+} germ cells are seen (arrows), especially around hub-like structures. GFP was simultaneously driven with Upd to control for dilution of the Gal4 by multiple UAS sites. **(B)** When Upd overexpression is combined with RNAi of the Dpp receptor Thickveins, tumors of GSC-like cells still form. Now, Mad is confined to cyst cells (arrows) and is not found in germ cells.

Scale bars, 10 μm.

A ***nos > tkv^{RNAi}, upd***

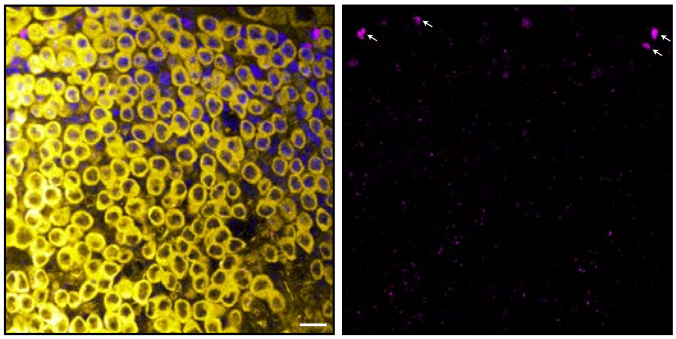

Supplemental Figure 4. Bmp and Jak-Stat tumors differ. (A) 3D reconstruction (see methods) of a Jak-Stat tumor (left) and a Bmp tumor (right). In the Jak-Stat tumor, fusomes (Adducin^{+} structures) are individual and small. In the Bmp tumor, fusomes have a large branched morphology. **(B)** Mitotic cells are marked by phosphorylated histone 3. In Bmp tumors, cells in a cyst enter meiosis synchronously. In Jak-Stat tumors, cells enter meiosis asynchronously with their neighbors.

Scale bars, 10 μm.

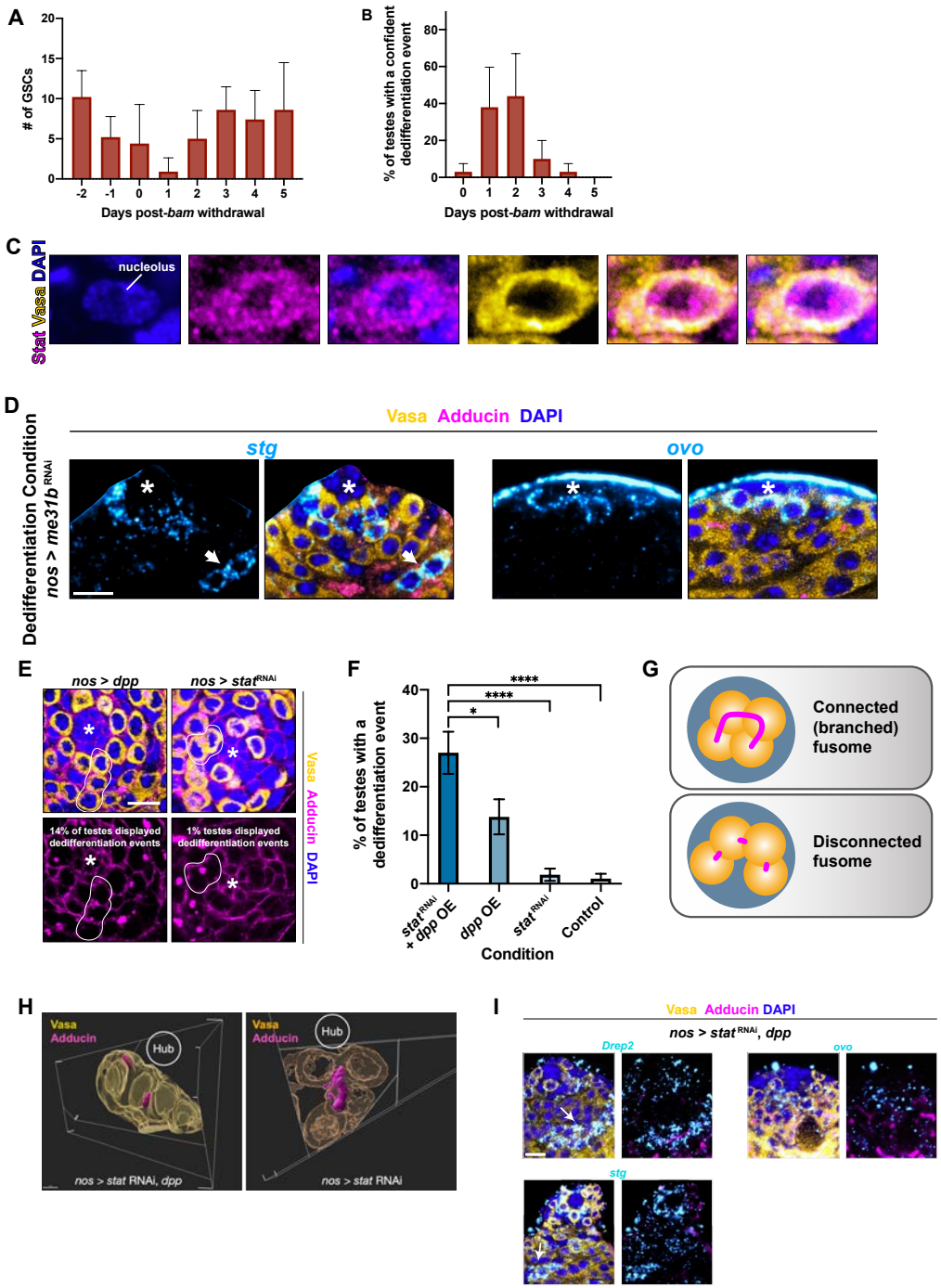

Supplemental Figure 5. Characterization of dedifferentiation conditions. (A) Quantification of GSC number in days after withdrawal of ectopic Bam. GSCs have depleted by day 1 post-withdrawal, and have returned to normal levels by day 3. Error bar, standard error. **(B)** Inset from **Fig 5A**. Stat signal in GSCs is both nuclear and cytoplasmic, but excluded from the nucleolus. Vasa signal is entirely cytoplasmic. **(C)** Quantification of "confident dedifferentiation events," as defined by ≥3 germ cells connected by fragmented fusomes contacting the hub.

Likely other dedifferentiation events exist that have not yet contacted the hub, and/or have not yet fragmented the fusome. Dedifferentiation events peak at approximately 2 days after withdrawal of ectopic Bam. **(D)** Dedifferentiation can be triggered by RNAi of *me31b*. In this condition, Bmp-sensitive transcript *stg* appears in spermatogonia outside its normal expression zone, but Bmp-insensitive transcript *ovo* does not. **(E)** Dpp tumor testes have an increased number of somatic hub cells and an increased number of GSCs[46]. In this condition, we observed 14% of testes with dedifferentiation events, as identified by ≥3 germ cells connected by fragmented fusomes contacting the hub (circled). Knockdown of *stat*, by contrast, leads to a reduced number of GSCs in the hub. However, we did not observe considerable dedifferentiation events above control, only asymmetric division events (circled). **(F)** Quantification of data in **Supp Fig 5D** and **Fig 5C**. First and last columns are also present in **Fig 5C**. Error bars, standard error. * $p<0.01$, **** $p<0.00001$, unpaired t-test. **(G)** Cartoon representation of spermatogonia with connected (branch) fusome and disconnected fusome. **(H)** 3D reconstruction of germ cells in $stat^{RNAi}$ and $stat^{RNAi}$, *dpp* conditions. In $stat^{RNAi}$, *dpp* testes, germ cells cysts adjacent to the hub had disconnected fusomes connecting ≥3 germ cells. In $stat^{RNAi}$ alone conditions, however, germ cell cysts contacting the hub had connected fusomes. This may suggest that Jak-Stat signaling plays a role in a return to GSC identity once the process of dedifferentiation has returned dedifferentiating spermatogonia to the hub. **(I)** *Drep2* and *stg* are both Bmp-sensitive transcripts and display expression outside of hub-adjacent GSCs in $stat^{RNAi}$, *dpp* conditions. *ovo*, by contrast, is Bmp-independent, and does not show such outside expression. *ovo* expression is also reduced in GSCs in this condition, suggesting some dependence on Jak-Stat signaling.

References Cited

1. Merrell, A. J. & Stanger, B. Z. Adult cell plasticity in vivo: De-differentiation and transdifferentiation are back in style. *Nat. Rev. Mol. Cell Biol.* **17**, 413–425 (2016).

2. Gehart, H. & Clevers, H. Tales from the crypt: new insights into intestinal stem cells. *Nat. Rev. Gastroenterol. Hepatol.* **16**, 19–34 (2019).

3. Nakagawa, T., Sharma, M., Nabeshima, Y., Braun, R. E. & Yoshida, S. Functional Hierarchy and Reversibility Within the Murine Spermatogenic Stem Cell Compartment. *Science* 62–68 (2010).

4. Kai, T. & Spradling, A. Differentiating germ cells can revert into functional stem cells in Drosophila melanogaster ovaries. *Nature* **428**, 564–569 (2004).

5. Sheng, X. R. & Matunis, E. Live imaging of the Drosophila spermatogonial stem cell niche reveals novel mechanisms regulating germline stem cell output. *Development* **138**, 3367–3376 (2011).

6. Rompolas, P., Mesa, K. R. & Greco, V. Spatial organization within a niche as a determinant of stem-cell fate. *Nature* **502**, 513–518 (2013).

7. Raven, A. *et al.* Cholangiocytes act as facultative liver stem cells during impaired hepatocyte regeneration. *Nature* **547**, 350–354 (2017).

8. Oderberg, I. M. & Goessling, W. Biliary epithelial cells are facultative liver stem cells during liver regeneration in adult zebrafish. *JCI Insight* **8**, (2023).

9. Lin, B. *et al.* Injury Induces Endogenous Reprogramming and Dedifferentiation of Neuronal Progenitors to Multipotency. *Cell Stem Cell* **21**, 761-774.e5 (2017).

10. Jopling, C. *et al.* Zebrafish heart regeneration occurs by cardiomyocyte dedifferentiation and proliferation. *Nature* **464**, 606–609 (2010).

11. Tata, P. R. *et al.* Dedifferentiation of committed epithelial cells into stem cells in vivo. *Nature* **503**, 218–223 (2013).

12. Friedmann-Morvinski, D. & Verma, I. M. Dedifferentiation and reprogramming: Origins of cancer stem cells. *EMBO Rep.* **15**, 244–253 (2014).

13. Greenspan, L. J., de Cuevas, M. & Matunis, E. Genetics of Gonadal Stem Cell Renewal. *Annu. Rev. Cell Dev. Biol.* **31**, 291–315 (2015).

14. Yamashita, Y. M., Jones, D. L. & Fuller, M. T. Orientation of asymmetric stem cell division by the APC tumor suppressor and centrosome. *Science* **301**, 1547–1550 (2003).

15. Yuan, H. & Yamashita, Y. M. Germline stem cells: Stems of the next generation. *Curr. Opin. Cell Biol.* **22**, 730–736 (2010).

16. Sheng, X. R., Brawley, C. M. & Matunis, E. L. Dedifferentiating Spermatogonia Outcompete Somatic Stem Cells for Niche Occupancy in the Drosophila Testis. *Cell Stem*

Cell **5**, 191–203 (2009).

17. Brawley, C. & Matunis, E. Regeneration of male germline stem cells by spermatogonial dedifferentiation in vivo. *Science* **304**, 1331–1334 (2004).

18. Herrera, S. C. & Bach, E. A. JNK signaling triggers spermatogonial dedifferentiation during chronic stress to maintain the germline stem cell pool in the drosophila testis. *Elife* **7**, 1–20 (2018).

19. Yang, H. & Yamashita, Y. M. The regulated elimination of transit-amplifying cells preserves tissue homeostasis during protein starvation in Drosophila testis. *Dev.* **142**, 1756–1766 (2015).

20. Cheng, J. *et al.* Centrosome misorientation reduces stem cell division during ageing. *Nature* **456**, 599–604 (2008).

21. Tran, V., Lim, C., Xie, J. & Chen, X. Asymmetric Division of Drosophila Male Germline Stem Cell Shows Asymmetric Histone Distribution. *Science* **338**, 679–682 (2012).

22. Watase, G. J., Nelson, J. O. & Yamashita, Y. M. Nonrandom sister chromatid segregation mediates rDNA copy number maintenance in Drosophila. *Sci. Adv.* **8**, 1–11 (2022).

23. Yamashita, Y. M., Mahowald, A. P., Perlin, J. R. & Fuller, M. T. Asymmetric inheritance of mother versus daughter centrosome in stem cell division. *Science* **315**, 518–521 (2007).

24. Yadlapalli, S. & Yamashita, Y. M. Chromosome-specific nonrandom sister chromatid segregation during stem-cell division. *Nature* **498**, 251–254 (2013).

25. Nelson, J. O., Kumon, T. & Yamashita, Y. M. rDNA magnification is a unique feature of germline stem cells. *Proc. Natl. Acad. Sci.* **120**, (2023).

26. Lu, K. L. & Yamashita, Y. M. Germ cell connectivity enhances cell death in response to DNA damage in the drosophila testis. *Elife* **6**, 1–16 (2017).

27. Lenhart, K. F. & DiNardo, S. Somatic Cell Encystment Promotes Abscission in Germline Stem Cells following a Regulated Block in Cytokinesis. *Dev. Cell* **34**, 192–205 (2015).

28. Raz, A. A. *et al.* Emergent dynamics of adult stem cell lineages from single nucleus and single cell RNA-Seq of Drosophila testes. *Elife* 2022.07.26.501581 (2023).

29. Trapnell, C. *et al.* The dynamics and regulators of cell fate decisions are revealed by pseudotemporal ordering of single cells. *Nat. Biotechnol.* **32**, 381–386 (2014).

30. Kharchenko, P. V., Silberstein, L. & Scadden, D. T. Bayesian approach to single-cell differential expression analysis. *Nat. Methods* **11**, 740–742 (2014).

31. Voog, J. *et al.* Escargot Restricts Niche Cell to Stem Cell Conversion in the Drosophila Testis. *Cell Rep.* **7**, 722–734 (2014).

32. Lapan, S. W. & Reddien, P. W. Transcriptome Analysis of the Planarian Eye Identifies ovo as a Specific Regulator of Eye Regeneration. *Cell Rep.* **2**, 1–14 (2012).

33. Takemura, M. *et al.* Drosophila MOV10 regulates the termination of midgut regeneration. *Genetics* **218**, (2021).

34. Lü, J., Andrews, J., Pauli, D. & Oliver, B. Drosophila OVO zinc-finger protein regulates ovo and ovarian tumor target promoters. *Dev. Genes Evol.* **208**, 213–222 (1998).

35. Inaba, M., Yuan, H. & Yamashita, Y. M. String (Cdc25) regulates stem cell maintenance, proliferation and aging in Drosophila testis. *Development* **138**, 5079–5086 (2011).

36. Tanentzapf, G., Devenport, D., Godt, D. & Brown, N. H. Integrin-dependent anchoring of a stem-cell niche. *Nat. Cell Biol.* **9**, 1413–1418 (2007).

37. Tootle, T. L. & Spradling, A. C. Drosophila Pxt: A cyclooxygenase-like facilitator of follicle maturation. *Development* **135**, 839–847 (2008).

38. Andlauer, T. F. M. *et al.* Drep-2 is a novel synaptic protein important for learning and memory. *Elife* **3**, 1–24 (2014).

39. Jensen, L. *et al.* me31B regulates stem cell homeostasis by preventing excess dedifferentiation in the Drosophila male germline . *J. Cell Sci.* **134**, (2021).

40. Tulina, N. & Matunis, E. Control of Stem Cell Self-Renewal in Drosophila Spermatogenesis by JAK-STAT Signaling. *Science* **294**, 2546–2549 (2001).

41. Kawase, E., Wong, M. D., Ding, B. C. & Xie, T. Gbb/Bmp signaling is essential for maintaining germline stem cells and for repressing bam transcription in the Drosophilatestis. *Development* **131**, 1365–1375 (2004).

42. Boyle, M., Wong, C., Rocha, M. & Jones, D. L. Decline in Self-Renewal Factors Contributes to Aging of the Stem Cell Niche in the Drosophila Testis. *Cell Stem Cell* **1**, 470–478 (2007).

43. Herrera, S. C. & Bach, E. A. JAK/STAT signaling in stem cells and regeneration: From drosophila to vertebrates. *Dev.* **146**, (2019).

44. Akiyama, T., Raftery, L. A. & Wharton, K. A. Bone morphogenetic protein signaling: the pathway and its regulation. *Genetics* **226**, 1–40 (2024).

45. Bener, M. B., Twillie, A. & Inaba, M. Dedifferentiating germ cells regain stem-cell specific polarity checkpoint prior to niche reentry. *bioRxiv Prepr. Serv. Biol.* (2023).

46. Schulz, C. *et al.* A misexpression screen reveals effects of bag-of-marbles and TGFβ class signaling on the Drosophila male germ-line stem cell lineage. *Genetics* **167**, 707–723 (2004).

47. Kiger, A., Leanne, J. D., Cordula, S., Rogers, M. & Fuller, M. Stem Cell Self-Renewal Specified by JAK-STAT Activation in Response to a Support Cell Cue. *Science* **294**, 2542–2545 (2001).

48. Wang, L., Li, Z. & Cai, Y. The JAK/STAT pathway positively regulates DPP signaling in

the Drosophila germline stem cell niche. *J. Cell Biol.* **180**, 721–728 (2008).

49. Kawase, E., Wong, M. D., Ding, B. C. & Xie, T. Gbb/Bmp signaling is essential for maintaining germline stem cells and for repressing bam transcription in the Drosophila testis. *Development* **131**, 1365–1375 (2004).

50. Greenbaum, M. P., Iwamori, T., Buchold, G. M. & Matzuk, M. M. Germ cell intercellular bridges. *Cold Spring Harb. Perspect. Biol.* **3**, 1–18 (2011).

51. Vogel, C. & Marcotte, E. M. Insights into the regulation of protein abundance from proteomic and transcriptomic analyses. *Nat. Rev. Genet.* **13**, 227–232 (2012).

52. Wang, R., Roiuk, M., Storer, F., Teleman, A. A. & Amoyel, M. Signals from the niche promote distinct modes of translation initiation to control stem cell differentiation and renewal in the Drosophila testis. 1–35 (2025) doi:10.1371/journal.pbio.3003049.

53. Inaba, M., Buszczak, M. & Yamashita, Y. M. Nanotubes mediate niche-stem-cell signalling in the Drosophila testis. *Nature* **523**, 329–332 (2015).

54. Harrison, D. A., Mccoon, P. E., Binari, R., Gilman, M. & Perrimon, N. Drosophila unpaired encodes a secreted protein that activates the JAK signaling pathway. *Genes Dev.* 1–12 (1998).

55. Ridwan, S. M. *et al.* Diffusible fraction of niche BMP ligand safeguards stem-cell differentiation. *Nat. Commun.* 1–17 (2023) doi:10.1038/s41467-024-45408-7.

56. Nellen, D., Burke, R., Struhl, G. & Basler, K. Direct and Long-Range Action of a DPP Morphogen Gradient. *Cell* **85**, 1–12 (1996).

57. Tomancak, P. *et al.* Systematic determination of patterns of gene expression during Drosophila embryogenesis. *Genome Biol.* **3**, RESEARCH0088 (2002).

58. Fingerhut, J. M. & Yamashita, Y. M. mRNA localization mediates maturation of cytoplasmic cilia in Drosophila spermatogenesis. *J. Cell Biol.* **219**, e202003084 (2020).